




Polarization dynamics of trapped polariton condensates with \mathcal{PT} symmetry

I. Jesan Velazquez-Resendiz  and Yuri G. Rubo ^{*}

Instituto de Energas Renovables, Universidad Nacional Autonoma de Mexico, Temixco, Morelos 62580, Mexico

 (Received 5 January 2024; revised 6 February 2024; accepted 7 February 2024; published 29 February 2024)

We propose a grated microcavity setup to form trapped polariton condensates with parity-time (\mathcal{PT}) symmetry and study their polarization dynamics. The pseudoconservative dynamics of the Stokes vector in the proposed configuration is preserved in the presence of a polariton-polariton interaction. In the case of weak gain-dissipation imbalance, as compared to the linear polarization splitting, the polarization Stokes spheres are deformed into ellipsoids. When linear polarization splitting becomes weak, i.e., when \mathcal{PT} symmetry is broken for a noninteracting system, the Stokes spheres are transformed into hyperboloids, but the dynamics is still described by closed trajectories, allowing manipulation of the polarization of the polariton condensate by changing the polarization splitting without losing its coherency.

DOI: [10.1103/PhysRevB.109.085312](https://doi.org/10.1103/PhysRevB.109.085312)

I. INTRODUCTION

The discovery of exciton-polariton condensation and lasing [1,2] marked an important milestone in modern nonlinear optics. Due to the excitonic component of a polariton quasi-particle, the space configuration of the condensates can be managed by pump and external fields, while the polarization of the condensate provides evidence of spontaneous symmetry breaking and monitors the dynamics of the order parameter [3–5]. Even in the simplest case of a single trapped polariton condensate, which is spatially disconnected from the reservoirs of incoherent exciton polaritons created by pumping [6,7], the polarization state can be rather nontrivial. It can exhibit the formation of a circular polarization degree with random handedness, manifesting the spontaneous breaking of parity [8]. Furthermore, the handedness can be manipulated by an applied electric field, which controls the splitting ε between X and Y linearly polarized states, which can be useful for computation with low-energy consumption [9].

While the polariton condensate is a driven-dissipative system, the symmetry breaking resulting in the spontaneous formation of circular polarization could be understood by considering the condensate as a conservative Hamiltonian system. In this approximation, the dynamics is mapped to that of the Bose-Hubbard dimer [10–14], or, if one uses the Schwinger realization of the angular momentum, to the dynamics of the Lipkin-Meshkov-Glick model [15,16], where the parity symmetry breaking is known as the formation of self-trapped many-body states [17,18]. The behavior of these systems, especially close to the long-period classical trajectories, has attracted much attention recently to study scrambling [19,20], quantum phase transitions [21], and possible applications for classical and quantum informatics.

Based on these features of polariton dimers, recently there is growing interest in the use of polariton condensates as

possible elements for classical and quantum computing [22]. The main obstacle comes from the fact that polariton condensates are dissipative systems, and to produce and maintain them it is necessary to apply external pumping, which easily destroys long-time coherence and related quantum effects such as entanglement between the condensates in a network. To apply polariton condensates for information and computation goals it is desirable to force the condensate to possess conservative or pseudoconservative dynamics. The latter is characterized by a continuum of closed orbits in the classical phase space, or by the real energy spectrum in the quantum limit. A promising method to achieve this is to form parity-time (\mathcal{PT}) symmetric polariton condensates [23,24].

Since the pioneering work by Bender and Boettcher [25], the non-Hermitian \mathcal{PT} -symmetric systems have attracted much attention both theoretically and experimentally (see Ref. [26] for a review). These systems can possess a real-valued energy spectrum if the \mathcal{PT} symmetry is unbroken, or pairs of complex-conjugate energy eigenvalues when the symmetry is spontaneously broken. The latter case is usually achieved for a big enough non-Hermitian part of the Hamiltonian. In a typical example of a two-state quantum system, characterized by the coherent coupling ε and dissipative coupling γ between the states, the \mathcal{PT} symmetry becomes broken for $|\gamma| > |\varepsilon|$, which is unwanted if one aims to manipulate the system state by an adiabatic change of ε . The account of a polariton-polariton interaction leads to nonlinear equations with even more complex behavior [27]. In particular, the spontaneous parity breaking in the case of a Bose-Hubbard dimer is accompanied by the suppression of time reversal [28]. This results in broken \mathcal{PT} symmetry even for a small dissipative coupling parameter, that is manifested by the blowup dynamics [29] with disclosed classical trajectories.

To overcome these difficulties, in this paper we propose and analyze a special grated microcavity setup that introduces a dissipation imbalance and polarization splitting between different linearly polarized states. This allows building the \mathcal{PT} -symmetric polariton condensates, and we demonstrate

^{*}ygr@ier.unam.mx

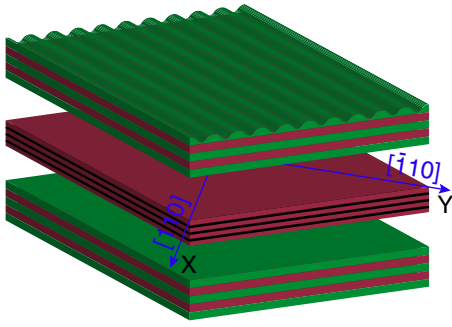


FIG. 1. Schematic view of the microcavity with subwavelength grating of one distributed Bragg mirror. The grating induces different dissipation rates for polaritons with diagonal [100] and antidiagonal [010] linear polarizations, while there is energy splitting between [110] (X direction) and $[\bar{1}10]$ (Y direction) linearly polarized polaritons.

the persistence of pseudoconservative dynamics even at high occupation levels, where the polariton-polariton interaction and related nonlinearities are important.

II. MICROCAVITY STRUCTURE AND THE MODEL

The polaritons in semiconductor microcavities, grown along the [001] direction, present a linear polarization dichroism, characterized by the splitting ε between the X (horizontal) and Y (vertical) linear polarizations, that are defined by the crystallographic [110] and $[\bar{1}10]$ axes, as shown in Fig. 1. This splitting appears mainly due to the mixture of the light- and the heavy-hole exciton components of a polariton wave function on the low-symmetry interfaces of the quantum wells [30–32]. The splitting is typically about tens of μeV .

Apart from the Hermitian splitting between the linear polarization components, we propose to introduce polarization-dependent dissipation. This can be achieved by weak subwavelength grating (SWG) of the microcavity surface, which makes reflectivity of the distributed Bragg mirror dependent on the polariton polarization [33,34]. To obtain a suitable dissipation imbalance one can use a microcavity grating along the diagonal or antidiagonal direction, i.e., along either the [100] or [010] direction. This introduces a difference in the lifetimes of polaritons with diagonal and antidiagonal polarizations. In this configuration, the single-polariton Hamiltonian describing the polarization state of a trapped polariton can be written in a circular polarization basis as

$$H_s = -\frac{1}{2} \begin{pmatrix} ig & \varepsilon - i\varepsilon' + \gamma \\ \varepsilon + i\varepsilon' - \gamma & ig \end{pmatrix}. \quad (1)$$

Here, $g = \Gamma - W$, where W is the external nonresonant pumping rate, Γ is the average dissipation rate, and γ defines the dissipation imbalance (we set $\hbar = 1$). In general, weak SWG induces an addition splitting, which we encoded in Eq. (1) by the parameter ε' . It is important to note that the Hermitian parts of the single-polariton Hamiltonian (1) can be tuned by an applied electric field [9] and by the strain [35,36], and in what follows, we assume that the additional splitting is removed, $\varepsilon' = 0$. The idea to introduce the coherent and dissipative couplings in the X and Y directions, respectively,

is to maintain the closed trajectories even in the presence of interactions. This happens because the spin orbits of the Bose-Hubbard dimer remain symmetric under the inversion $y \rightarrow -y$.

As a result, when the external pump of the condensate matches the average dissipation from the microcavity, i.e., $g = 0$, the condensate is described by the \mathcal{PT} -symmetric Hamiltonian $H_{s0} = -(\varepsilon\sigma_x + i\gamma\sigma_y)/2$ with the energies $\pm\sqrt{\varepsilon^2 - \gamma^2}/2$. The general description of the 2×2 \mathcal{PT} -symmetric matrices can be found in Ref. [37]. In our case, the parity operation is defined by the Pauli x matrix, $\mathcal{P} = \sigma_x$, while the time-reversal operation is $\mathcal{T} = K\sigma_x$, where K is the complex conjugation, so that any real matrix is in fact \mathcal{PT} symmetric. Note that the time inversion, apart from complex conjugation, also exchanges the circular polarization components. It is worth noting also that the Hamiltonian (1) describes as well the asymmetric hopping between two localized states, which for the case of a chain of such states is known as the Hatano-Nelson model [38].

The many-body extension of our model accounts for the interaction of polaritons with the same circular polarization, which corresponds to the following equations,

$$i\frac{d\hat{\psi}_{\pm 1}}{dt} = -\frac{1}{2}(\varepsilon \pm \gamma)\hat{\psi}_{\mp 1} + \frac{\alpha}{2}\hat{\psi}_{\pm 1}^\dagger\hat{\psi}_{\pm 1}^2, \quad (2)$$

for the dynamics of the annihilation operators of polaritons with right (+1) and the left (-1) circular polarizations, where α is the interaction constant. It is convenient to introduce the spin operators as $\hat{s}_k = \frac{1}{2}(\Psi^\dagger \cdot \sigma_k \cdot \Psi)$ for $k = 0, x, y, z$, where the column vector $\Psi = (\hat{\psi}_{+1}, \hat{\psi}_{-1})^\top$, $\sigma_{x,y,z}$ are the Pauli matrices, and σ_0 is the 2×2 identity matrix. The spin dynamics is then governed by the equations

$$\frac{d\hat{s}_0}{dt} = -\gamma\hat{s}_y, \quad \frac{d\hat{s}_x}{dt} = -\frac{\alpha}{2}\{\hat{s}_z, \hat{s}_y\}, \quad (3a)$$

$$\frac{d\hat{s}_y}{dt} = -\gamma\hat{s}_0 + \varepsilon\hat{s}_z + \frac{\alpha}{2}\{\hat{s}_z, \hat{s}_x\}, \quad \frac{d\hat{s}_z}{dt} = -\varepsilon\hat{s}_y, \quad (3b)$$

where $\{\hat{s}_k, \hat{s}_l\} = \hat{s}_k\hat{s}_l + \hat{s}_l\hat{s}_k$.

It is easy to see that the single-polariton energies are real and the \mathcal{PT} symmetry is unbroken for $|\varepsilon| > |\gamma|$, and it is important to note that the presence of a polariton-polariton interaction does not change this fact. The non-Hermitian Bose-Hubbard Hamiltonian that corresponds to Eq. (2) is

$$\hat{\mathcal{H}} = -\frac{(\varepsilon + \gamma)}{2}\hat{\psi}_{+1}^\dagger\hat{\psi}_{-1} - \frac{(\varepsilon - \gamma)}{2}\hat{\psi}_{-1}^\dagger\hat{\psi}_{+1} + \frac{\alpha}{4}[\hat{\psi}_{+1}^\dagger\hat{\psi}_{+1}^2 + \hat{\psi}_{-1}^\dagger\hat{\psi}_{-1}^2], \quad (4)$$

or, using the spin operators,

$$\mathcal{H} = H_0(\hat{\mathbf{s}}) + iH_1(\hat{\mathbf{s}}), \quad (5a)$$

$$H_0(\hat{\mathbf{s}}) = -\varepsilon\hat{s}_x + \frac{\alpha}{2}[\hat{s}_z^2 + \hat{s}_0^2 - \hat{s}_0], \quad (5b)$$

$$H_1(\hat{\mathbf{s}}) = -\gamma\hat{s}_y. \quad (5c)$$

This Hamiltonian can be transformed into an Hermitian operator by the Dyson transformation $e^{-t\hat{s}_z}\mathcal{H}e^{t\hat{s}_z}$ with $\tanh(t) = \gamma/\varepsilon$, which eliminates the H_1 part and renormalizes the Josephson coupling parameter to $\tilde{\varepsilon} = \sqrt{\varepsilon^2 - \gamma^2}$.

In the opposite case, $|\varepsilon| < |\gamma|$, the \mathcal{PT} symmetry is broken and the single-polariton energies becomes complex. Including the polariton-polariton interaction actually improves the situation. As we show below in the mean-field approximation valid for large occupation numbers, this model preserves pseudo-conservative dynamics even for small splittings ε .

III. SEMICLASSICAL DYNAMICS

In the mean-field approximation, the spin operator $\hat{\mathbf{s}} = \{\hat{s}_x, \hat{s}_y, \hat{s}_z\}$ is replaced by a three-dimensional (3D) vector \mathbf{S} with the length $S = \sqrt{S_x^2 + S_y^2 + S_z^2}$. The length is not conserved in our case and the spin satisfies the dynamical equation

$$\frac{d\mathbf{S}}{dt} = \left[\frac{dH_0}{d\mathbf{S}} \times \mathbf{S} \right] + S \frac{dH_1}{d\mathbf{S}}, \quad (6)$$

or, in the components,

$$\dot{S}_x = -\alpha S_z S_y, \quad \dot{S}_y = -\gamma S + \varepsilon S_z + \alpha S_z S_x, \quad (7a)$$

$$\dot{S}_z = -\varepsilon S_y, \quad \dot{S} = -\gamma S_y. \quad (7b)$$

In what follows, we will assume that the parameters α , γ , and ε have positive values. In the case of negative values, one can reestablish Eqs. (7a) and (7b) with positive parameters by using appropriate transformations of the spin components. For example, in the case of an attractive interaction, $\alpha < 0$, we apply $S_x \rightarrow -S_x$. In the case of $\varepsilon < 0$ we apply $S_z \rightarrow -S_z$ together with $S_x \rightarrow -S_x$. Finally, in the case of $\gamma < 0$ we invert $S_z \rightarrow -S_z$ and $S_y \rightarrow -S_y$. By choosing ε^{-1} as the unit of time we can always set $\varepsilon = 1$, and we also can rescale the spin $\alpha \mathbf{S} = \mathbf{s} = \{x, y, z\}$ to obtain

$$\dot{x} = -zy, \quad \dot{y} = -\gamma s + z + zx, \quad (8a)$$

$$\dot{z} = -y, \quad \dot{s} = -\gamma y. \quad (8b)$$

The system of equations (8) has two integrals of motion, the ‘‘energy’’ E and the parameter ρ , that defines the spin size:

$$E = -x + \frac{1}{2}z^2, \quad \rho = s - \gamma z. \quad (9)$$

Applying these invariants we obtain the following equation for the z component,

$$\begin{aligned} \left(\frac{dz}{dt} \right)^2 &= (\rho + \gamma z)^2 - \left(\frac{z^2}{2} - E \right)^2 - z^2 \\ &= -\frac{1}{4}(z - z_1)(z - z_2)(z - z_3)(z - z_4), \end{aligned} \quad (10)$$

where instead of the parameters E , ρ , γ we also defined the four roots $z_{1,2,3,4}$ of the quartic polynomial in the right-hand side. They are subject to $z_1 + z_2 + z_3 + z_4 = 0$.

Equation (10) can be solved analytically using a Möbius (homographic) transformation

$$w(t) = \frac{az(t) + b}{cz(t) + d}, \quad (11)$$

and adjusting the constants a, b, c, d to obtain the equation for the Jacobi elliptic cosine function $w(t) = \pm \text{cn}(\omega t, m)$,

$$\left(\frac{dw}{dt} \right)^2 = -m\omega^2(w^2 - w_0^2)(w^2 - 1), \quad w_0^2 = \frac{m-1}{m}, \quad (12)$$

similar to discussion in Ref. [39]. In our case, special care should be taken concerning the number of real roots, since one can have either all four real roots $z_{1,2,3,4}$ or only two real roots and a pair of complex ones.

Consider the case of four real roots $z_1 < z_2 < z_3 < z_4$. The coefficients of the Möbius transformation can be found from the mapping of the fixed points of Eqs. (10) and (12) as $z_i \leftrightarrow w_i, i = 1, 2, 3, 4$, with

$$w_1 = -1, \quad w_2 = -w_0, \quad w_3 = w_0, \quad w_4 = 1. \quad (13)$$

Note that it is necessary to have a real w_0 that corresponds to $m > 1$. The parameters m and ω are then obtained from the condition of conservation of the cross ratio for the Möbius transformation:

$$\frac{(z_1 - z_4)(z_2 - z_3)}{(z_1 - z_3)(z_2 - z_4)} = \frac{(w_1 - w_4)(w_2 - w_3)}{(w_1 - w_3)(w_2 - w_4)} = \frac{4w_0}{(1 + w_0)^2}. \quad (14)$$

As a result, the solution to (10) can be written as

$$z(t) = \frac{\omega_1 z_4 [1 \pm \text{cn}(\omega t, m)] + \omega_4 z_1 [1 \mp \text{cn}(\omega t, m)]}{\omega_1 [1 \pm \text{cn}(\omega t, m)] + \omega_4 [1 \mp \text{cn}(\omega t, m)]}, \quad (15)$$

where

$$\omega_1 = \sqrt{(z_1 - z_2)(z_1 - z_3)}, \quad \omega_4 = \sqrt{(z_3 - z_4)(z_2 - z_4)}, \quad (16a)$$

$$\omega = \frac{1}{2} \sqrt{\omega_1 \omega_4}, \quad m = \frac{[\omega_1 \omega_4 + (z_1 - z_2)(z_3 - z_4)]^2}{4\omega_1 \omega_4 (z_1 - z_2)(z_3 - z_4)} \quad (16b)$$

The above expressions remain valid for the case when there are only two real roots, if they are chosen as $z_1 < z_4$, while $z_2 = z_3^*$. The modulus of the elliptic cosine function $m < 1$ in this case, $\text{cn}(\omega t, m)$ oscillates between ± 1 , and the upper and lower signs in (15) describe the same solution, which oscillates between z_1 and z_4 . On the other hand, in the case of four real roots, the modulus $m > 1$ and $\text{cn}(\omega t, m) = \text{dn}(\sqrt{m} \omega t, 1/m)$ oscillates between 1 and $w_0 = \sqrt{m-1}/m$, so that the upper sign in (15) describes oscillations between z_3 and z_4 , while the lower sign corresponds to oscillations between z_1 and z_2 . Finally, knowing $z(t)$ one can calculate $x(t) = (1/2)z(t)^2 - E$, and using $y = -\dot{z}$ obtain

$$y(t) = \pm \frac{8\omega^3(z_4 - z_1) \text{dn}(\omega t, m) \text{sn}(\omega t, m)}{(\omega_1 [1 \pm \text{cn}(\omega t, m)] + \omega_4 [1 \mp \text{cn}(\omega t, m)])^2}. \quad (17)$$

The system under consideration possesses the closed, pseudo-conservative trajectories only. This is in sharp contrast to the other possible \mathcal{PT} -symmetric configurations. For example, another way to add a non-Hermitian \mathcal{PT} -symmetric part to the Hamiltonian is to introduce the pump-dissipation imbalance between the circular components, which corresponds to $H_1(\hat{\mathbf{s}}) = -\gamma \hat{s}_z$. The resulting semiclassical dynamics of the dimer is characterized by disclosed blowup trajectories and, therefore, by broken \mathcal{PT} symmetry [29]. While the dynamics

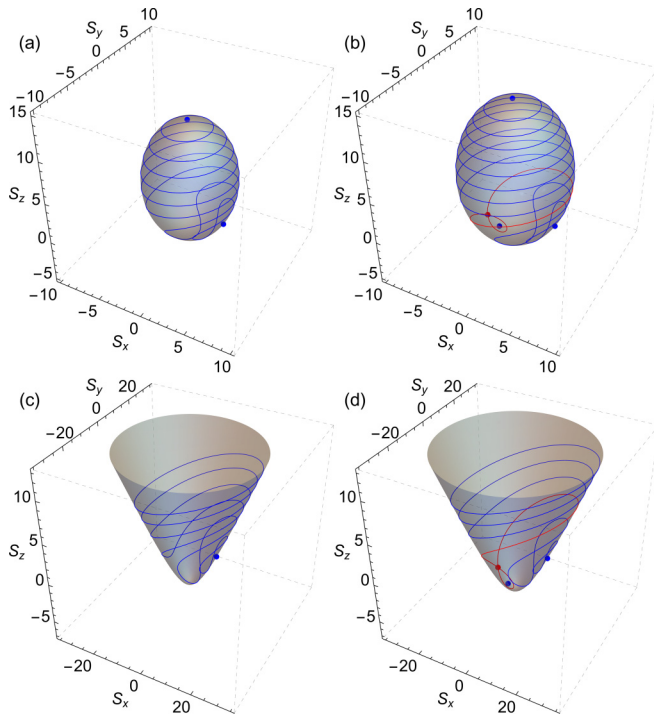


FIG. 2. Different topologies of the manifolds of spin trajectories. Showing weak dissipative coupling cases with $\gamma/\varepsilon = 0.7$ that leads to $\rho_c = 3.741$, with (a) $\rho = 3.6$ and (b) $\rho = 4.3$, corresponding to the spin moving on ellipsoids, and strong dissipative coupling cases with $\gamma/\varepsilon = 1.6$ that gives $\rho_c = 8.729$, with (c) $\rho = 8.5$ and (d) $\rho = 10.7$, corresponding to the motion on hyperboloids. The fixed points of the focus type are shown in blue, while the saddle points and the saddle trajectories are plotted in red.

is pseudoconservative in our case, there is a qualitative change in the topology of the manifold of trajectories with increasing dissipation imbalance γ . As shown in Fig. 2, the trajectories reside on the spindle-shaped ellipsoids (prolate spheroids) for $\gamma < \varepsilon$, and on the upper sheets of the two-sheet hyperboloids for $\gamma > \varepsilon$. Note that the lower sheets of these hyperboloids are fictitious, so they do not represent valid manifolds of spin trajectories.

Another important feature is the change in the number of fixed points with increasing size of the ellipsoids or the hyperboloids. The size is controlled by the integral ρ . One can find the fixed points by setting the time derivatives to zero in Eqs. (8), which gives

$$y = 0, \quad z = \frac{\gamma\rho}{1 - \gamma^2 + x}, \quad (18a)$$

$$(1 - \gamma^2 + x)^2 x^2 - \rho^2 [(1 + x)^2 - \gamma^2] = 0. \quad (18b)$$

A standard analysis of the discriminant of Eq. (18b) reveals that this equation has two real roots for $\rho < \rho_c$, and four real roots for $\rho > \rho_c$. The critical size ρ_c is

$$\rho_c = [1 + \gamma^{2/3} + \gamma^{4/3}]^{3/2}. \quad (19)$$

This is exactly what happens in the case of weak dissipation imbalance ($\gamma < 1$). There are two fixed points of the focus type for $0 < \rho < \rho_c$, as shown in Fig. 2(a). Two more fixed points appear due to the saddle-node bifurcation at $\rho = \rho_c$.

The new focus and the saddle point initially appear at the same spin value, and they separate from each other with increasing ρ [see Fig. 2(b)]. A similar bifurcation takes place in the hyperbolic case ($\gamma > 1$). We note that ρ can be negative in the hyperbolic case and one real root of Eq. (18b) is fictitious, so that there is only one focus below ρ_c and three fixed points above it [see Figs. 2(c) and 2(d)]. Exactly at $\gamma = 1$, the spin trajectories reside on paraboloids, with one and three fixed points below and above $\rho_c = \sqrt{27}$, respectively.

We note that there are two saddle trajectories related to the presence of a saddle point [see Figs. 2(b) and 2(d)]. The time to go around the saddle trajectory is infinite. The periods of the spin orbits nearby are logarithmically large. Saddle trajectories correspond to the degeneracy of two roots of the quartic polynomial on the right-hand side of Eq. (10): $z_2 = z_3 = z_s$ with $z_1 < z_s < z_4$. In this case the modulus $m = 1$, $\omega_1 = z_s - z_1$, $\omega_4 = z_4 - z_s$, and $\text{cn}(\omega t, 1) = 1/\cosh(\omega t)$. Equation (15) then gives two solutions that start from the saddle point z_s at $t \rightarrow -\infty$, pass through either z_1 or z_4 at $t = 0$, and return to the saddle point at $t \rightarrow +\infty$.

IV. DISCUSSION AND CONCLUSIONS

Generally speaking, nonresonantly excited polariton condensates are open systems obeying nonlinear dissipative dynamics. Apart from typical wave phenomena, which are sometimes interpreted using quantum language, their behavior is within the classical concepts. Truly quantum features, such as entanglement, are not yet evidenced experimentally. To obtain the polariton dynamics that resembles that of the closed conservative systems, with possible quantum effects, it is necessary to detach the polariton condensates from the excitation spots of incoherent polariton reservoirs and decrease the shot noise produced by the harvest of polaritons by the condensate. This can be achieved close to the condensation threshold, and it is preferential to have a distribution of dissipation rates in the system, so that one obtains a threshold range, where the external pump can be adjusted.

The distribution of dissipation rates depending on polarization of a trapped polariton condensate can be achieved by using weakly grating microcavities (Fig. 1). We proposed to use a special configuration, where the Hermitian Josephson splitting ε and the non-Hermitian splitting in dissipation rates γ are introduced between different linear polarization pairs: horizontal-vertical and diagonal-antidiagonal, respectively. This way one can produce a trapped polariton condensate subject to a \mathcal{PT} -symmetric Hamiltonian. Moreover, we have shown that, at least in a semiclassical approximation, the \mathcal{PT} symmetry remains unbroken in the presence of a polariton-polariton repulsive interaction.

The dynamics of a \mathcal{PT} -symmetric polariton condensate is characterized by closed pseudoconservative trajectories, which opens the perspective to use it as a coherent qubit. The analytical expressions for the trajectories are derived. We have analyzed the bifurcations of the fixed points of this system and the crossover in the topology of the manifolds of trajectories. At a weak dissipation imbalance, $\gamma < \varepsilon$, the spin of the condensate precesses on the spindle-shaped ellipsoids, which is topologically equivalent to the usual spin precession on a sphere. For a large dissipation imbalance, however, the

precession takes place on hyperboloids and there is a decrease in the number of fixed points by one. The dynamics of large spins is featured by the presence of saddle trajectories. In the vicinity of them, the motion is slow with large periods of precession. The rich spin dynamics of \mathcal{PT} -symmetric trapped polariton condensates and the bifurcations of the fixed points make this platform promising for classical computation and neuromorphic simulations. To establish the possibility of quantum computation, an additional analysis of the decoherence due to the environment and of the effects of noise should be done in the framework of a fully quantum description.

The main signature of the formation of a \mathcal{PT} -symmetric polariton condensate is the coexistence of different dynamical states. The switching between them is expected to be slow, as

far as the noise is weak. Experimentally, this regime should be manifested by the formation of several distinct lines in the spectrum, demonstrating the superposition of emission coming from different fixed points, not just a single lasing line, with possible frequency combs appearing due to long-living periodic spin orbits.

ACKNOWLEDGMENTS

This work was supported in part by PAPIIT-UNAM Grant No. IN108524. The authors would like to thank the Institut Henri Poincaré (UAR 839 CNRS-Sorbonne Université) and the LabEx CARMIN (ANR-10-LABX-59-01) for their support.

-
- [1] J. Kasprzak, M. Richard, S. Kundermann, A. Baas, P. Jeambrun, J. M. J. Keeling, F. M. Marchetti, M. H. Szymańska, R. André, J. L. Staehli, V. Savona, P. B. Littlewood, B. Deveaud, and L. S. Dang, Bose-Einstein condensation of exciton polaritons, *Nature (London)* **443**, 409 (2006).
- [2] R. Balili, V. Hartwell, D. Snoke, L. Pfeiffer, and K. West, Bose-Einstein condensation of microcavity polaritons in a trap, *Science* **316**, 1007 (2007).
- [3] J. J. Baumberg, A. V. Kavokin, S. Christopoulos, A. J. D. Grundy, R. Butté, G. Christmann, D. D. Solnyshkov, G. Malpuech, G. Baldassarri Höger von Högersthal, E. Feltin, J.-F. Carlin, and N. Grandjean, Spontaneous polarization buildup in a room-temperature polariton laser, *Phys. Rev. Lett.* **101**, 136409 (2008).
- [4] J. Levrat, R. Butté, T. Christian, M. Glauser, E. Feltin, J.-F. Carlin, N. Grandjean, D. Read, A. V. Kavokin, and Y. G. Rubo, Pinning and depinning of the polarization of exciton-polariton condensates at room temperature, *Phys. Rev. Lett.* **104**, 166402 (2010).
- [5] D. Colas, L. Dominici, S. Donati, A. A. Pervishko, T. C. H. Liew, I. A. Shelykh, D. Ballarini, M. de Giorgi, A. Bramati, G. Gigli, E. del Valle, F. P. Laussy, A. V. Kavokin, and D. Sanvitto, Polarization shaping of Poincaré beams by polariton oscillations, *Light: Sci. Appl.* **4**, e350 (2015).
- [6] A. Askitopoulos, H. Ohadi, A. V. Kavokin, Z. Hatzopoulos, P. G. Savvidis, and P. G. Lagoudakis, Polariton condensation in an optically induced two-dimensional potential, *Phys. Rev. B* **88**, 041308(R) (2013).
- [7] P. Cristofolini, A. Dreismann, G. Christmann, G. Franchetti, N. G. Berloff, P. Tsotsis, Z. Hatzopoulos, P. G. Savvidis, and J. J. Baumberg, Optical superfluid phase transitions and trapping of polariton condensates, *Phys. Rev. Lett.* **110**, 186403 (2013).
- [8] H. Ohadi, A. Dreismann, Y. G. Rubo, F. Pinsker, Y. del Valle-Inclan Redondo, S. I. Tsintzos, Z. Hatzopoulos, P. G. Savvidis, and J. J. Baumberg, Spontaneous spin bifurcations and ferromagnetic phase transitions in a spinor exciton-polariton condensate, *Phys. Rev. X* **5**, 031002 (2015).
- [9] A. Dreismann, H. Ohadi, Y. del Valle-Inclan Redondo, R. Balili, Y. G. Rubo, S. I. Tsintzos, G. Deligeorgis, Z. Hatzopoulos, P. G. Savvidis, and J. J. Baumberg, A sub-femtojoule electrical spin-switch based on optically trapped polariton condensates, *Nat. Mater.* **15**, 1074 (2016).
- [10] A. Smerzi, S. Fantoni, S. Giovanazzi, and S. R. Shenoy, Quantum coherent atomic tunneling between two trapped Bose-Einstein condensates, *Phys. Rev. Lett.* **79**, 4950 (1997).
- [11] G. J. Milburn, J. Corney, E. M. Wright, and D. F. Walls, Quantum dynamics of an atomic Bose-Einstein condensate in a double-well potential, *Phys. Rev. A* **55**, 4318 (1997).
- [12] R. Franzosi and V. Penna, Spectral properties of coupled Bose-Einstein condensates, *Phys. Rev. A* **63**, 043609 (2001).
- [13] M. Albiez, R. Gati, J. Fölling, S. Hunsmann, M. Cristiani, and M. K. Oberthaler, Direct observation of tunneling and nonlinear self-trapping in a single bosonic Josephson junction, *Phys. Rev. Lett.* **95**, 010402 (2005).
- [14] T. Zibold, E. Nicklas, C. Gross, and M. K. Oberthaler, Classical bifurcation at the transition from Rabi to Josephson dynamics, *Phys. Rev. Lett.* **105**, 204101 (2010).
- [15] H. J. Lipkin, N. Meshkov, and A. J. Glick, Validity of many-body approximation methods for a solvable model: (I). Exact solutions and perturbation theory, *Nucl. Phys.* **62**, 188 (1965).
- [16] A. Vardi and J. R. Anglin, Bose-Einstein condensates beyond mean field theory: Quantum backreaction as decoherence, *Phys. Rev. Lett.* **86**, 568 (2001).
- [17] M. Holthaus and S. Stenholm, Coherent control of the self-trapping transition, *Eur. Phys. J. B* **20**, 451 (2001).
- [18] T. Pudlik, H. Hennig, D. Witthaut, and D. K. Campbell, Tunneling in the self-trapped regime of a two-well Bose-Einstein condensate, *Phys. Rev. A* **90**, 053610 (2014).
- [19] T. Xu, T. Scaffidi, and X. Cao, Does scrambling equal chaos? *Phys. Rev. Lett.* **124**, 140602 (2020).
- [20] S. Pilatowsky-Cameo, J. Chávez-Carlos, M. A. Bastarrachea-Magnani, P. Stránský, S. Lerma-Hernández, L. F. Santos, and J. G. Hirsch, Positive quantum Lyapunov exponents in experimental systems with a regular classical limit, *Phys. Rev. E* **101**, 010202(R) (2020).
- [21] Q. Wang and F. Pérez-Bernal, Probing an excited-state quantum phase transition in a quantum many-body system via an out-of-time-order correlator, *Phys. Rev. A* **100**, 062113 (2019).
- [22] A. Kavokin, T. C. H. Liew, C. Schneider, P. G. Lagoudakis, S. Klemmt, and S. Hoeffling, Polariton condensates for classical and quantum computing, *Nat. Rev. Phys.* **4**, 435 (2022).
- [23] I. Chestnov, Y. G. Rubo, A. Nalitov, and A. Kavokin, Pseudo-conservative dynamics of coupled polariton condensates, *Phys. Rev. Res.* **3**, 033187 (2021).

- [24] P. A. Kalozoumis and D. Petrosyan, Self-organized PT -symmetry of exciton-polariton condensate in a double-well potential, *Appl. Sci.* **11**, 7372 (2021).
- [25] C. M. Bender and S. Boettcher, Real spectra in non-Hermitian Hamiltonians having \mathcal{PT} symmetry, *Phys. Rev. Lett.* **80**, 5243 (1998).
- [26] C. M. Bender, P. E. Dorey, C. Dunning, A. Fring, D. W. Hook, H. F. Jones, S. Kuzhel, G. Lévai, and R. Tateo, *PT Symmetry: In Quantum and Classical Physics* (World Scientific, London, 2019).
- [27] V. V. Konotop, J. Yang, and D. A. Zezyulin, Nonlinear waves in \mathcal{PT} -symmetric systems, *Rev. Mod. Phys.* **88**, 035002 (2016).
- [28] A. A. Sukhorukov, Z. Xu, and Y. S. Kivshar, Nonlinear suppression of time reversals in \mathcal{PT} -symmetric optical couplers, *Phys. Rev. A* **82**, 043818 (2010).
- [29] I. V. Barashenkov, G. S. Jackson, and S. Flach, Blow-up regimes in the \mathcal{PT} -symmetric coupler and the actively coupled dimer, *Phys. Rev. A* **88**, 053817 (2013).
- [30] I. L. Aleiner and E. L. Ivchenko, Anisotropic exchange splitting in type-II GaAs/AlAs superlattices, *Pis'ma Zh. Eksp. Teor. Fiz.* **55**, 662 (1992) [*JETP Lett.* **55**, 692 (1992)].
- [31] E. L. Ivchenko, A. Y. Kaminski, and U. Rössler, Heavy-light hole mixing at zinc-blende (001) interfaces under normal incidence, *Phys. Rev. B* **54**, 5852 (1996).
- [32] G. Malpuech, M. M. Glazov, I. A. Shelykh, P. Bigenwald, and K. V. Kavokin, Electronic control of the polarization of light emitted by polariton lasers, *Appl. Phys. Lett.* **88**, 111118 (2006).
- [33] M. C. Y. Huang, Y. Zhou, and C. J. Chang-Hasnain, A surface-emitting laser incorporating a high-index-contrast sub-wavelength grating, *Nat. Photon.* **1**, 119 (2007).
- [34] S. Kim, B. Zhang, Z. Wang, J. Fischer, S. Brodbeck, M. Kamp, C. Schneider, S. Höfling, and H. Deng, Coherent polariton laser, *Phys. Rev. X* **6**, 011026 (2016).
- [35] Ł. Kłopotowski, M. D. Martín, A. Amo, L. Viña, I. A. Shelykh, M. M. Glazov, G. Malpuech, A. V. Kavokin, and R. André, Optical anisotropy and pinning of the linear polarization of light in semiconductor microcavities, *Solid State Commun.* **139**, 511 (2006).
- [36] R. Balili, B. Nelsen, D. W. Snoke, R. H. Reid, L. Pfeiffer, and K. West, Huge splitting of polariton states in microcavities under stress, *Phys. Rev. B* **81**, 125311 (2010).
- [37] Q.-H. Wang, 2×2 PT -symmetric matrices and their applications, *Philos. Trans. R. Soc. A* **371**, 20120045 (2013).
- [38] N. Hatano and D. R. Nelson, Localization transitions in non-Hermitian quantum mechanics, *Phys. Rev. Lett.* **77**, 570 (1996).
- [39] W. A. Schwalm, *Lectures on Selected Topics in Mathematical Physics: Elliptic Functions and Elliptic Integrals* (Morgan & Claypool, San Rafael, CA, 2015), Chap. 3.